JOC The Journal of Organic Chemistry

Article

pubs.acs.org/joc

Chemical Reactivity in Nucleophilic Cycloaddition to C_{70}: Vibronic Coupling Density and Vibronic Coupling Constants as Reactivity Indices

Naoki Haruta, Tohru Sato,* and Kazuyoshi Tanaka

Department of Molecular Engineering, Graduate School of Engineering, Kyoto University, Nishikyo-ku, Kyoto 615-8510, Japan

Supporting Information

ABSTRACT: The chemical reactivity in nucleophilic cycloaddition to C_{70} is investigated on the basis of vibronic (electron-vibration) coupling density and vibronic coupling constants. Because the e_1'' LUMOs of C_{70} are doubly degenerate and delocalized throughout the molecule, it is difficult to predict the regioselectivity by frontier orbital theory. It is found that vibronic coupling density analysis for the effective mode as a reaction mode illustrates the idea of a functional group embedded in the reactive sites. Furthermore, the vibronic coupling constants for localized stretching vibrational modes enable us to estimate the quantitative reactivity. These calculated results agree well with the experimental findings. The principle of chemical reactivity proposed by Parr and Yang is modified as follows: the preferred direction is the one for which the initial vibronic coupling density for a reaction mode of the isolated reactant is a minimum.

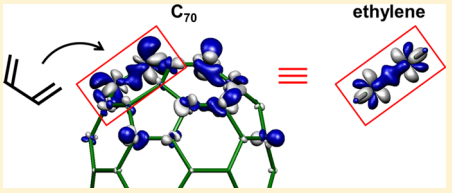

1. INTRODUCTION

C_{70} (Figure 1) is the second most abundant fullerene. To functionalize C_{70}, cycloaddition reactions have been widely

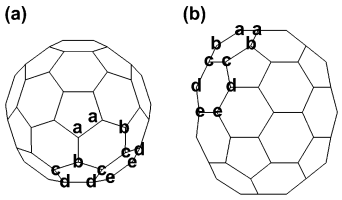

Figure 1. The geometry of C_{70} (D_{5h} symmetry): (a) top view, (b) side view.

investigated. Further, the chemical reactivity of this fullerene has attracted much attention in materials chemistry.[1] According to experimental findings, nucleophilic cycloadditions to C_{70} occur at the a−b bonds and c−c bonds (see Figure 1).[2,3] Further, the a−b bonds are known to be more than twice as reactive as the c−c bonds.

Because the e_1'' LUMOs and the a_1'' next LUMO are low-lying as shown in Figure 2, C_{70} is a good electron acceptor, comparable to C_{60}. According to frontier orbital theory,[4,5] the regioselectivity of C_{70} should be predicted by the LUMOs, and in some cases, by the nearly degenerate next LUMO (Figure 3). Since the LUMOs of C_{70} are doubly degenerate, their orbital patterns cannot be determined uniquely. For visualization, we can choose either the symmetrized set ($e_1''\theta$ LUMO, $e_1''\varepsilon$ LUMO) shown in Figure 3 or their unitarily transformed mixture. However, to discuss any observable effect such as reactivity on the basis of such degenerate orbitals, we should employ some invariant quantity under any unitary trans-

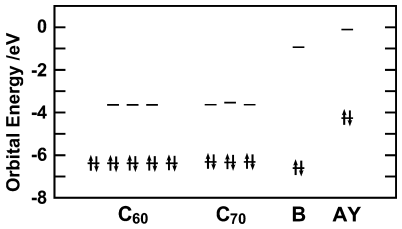

Figure 2. Frontier orbital levels of C_{60}, C_{70}, gauche butadiene (B), and *N*-methylazomethine ylide (AY) by RB3LYP/6-311G(d,p).

formation. Therefore, the averaged LUMO density should be used for these discussions (Figure 4). The averaged LUMO density is delocalized throughout the molecule except in the equatorial regions (e−e bonds), and it assumes the maximum value on the five-membered rings (a−a bonds), as shown in Figure 4. Experimental results show that the a−a bonds have very low reactivity. Moreover, the next LUMO has very small distribution at the most reactive sites (a−b bonds), as shown in Figure 3 (c1 and c2). Thus, the prediction from the frontier orbital density is clearly contradictory to the experimental findings. Therefore, it is difficult to predict the regioselectivity of C_{70} on the basis of frontier orbital theory.

Vibronic (electron-vibration) couplings[6,7] cause molecular distortions in the early stage of a chemical reaction and hence are worthy of being taken into consideration in addition to frontier orbital interactions. In this study, to predict the regioselectivity of C_{70}, we employ the concept of vibronic coupling density for a reaction mode.[8,9] Recently, we have

Received: August 21, 2012
Published: October 10, 2012

   dx.doi.org/10.1021/jo301777d | J. Org. Chem. 2012, 77, 9702−9706

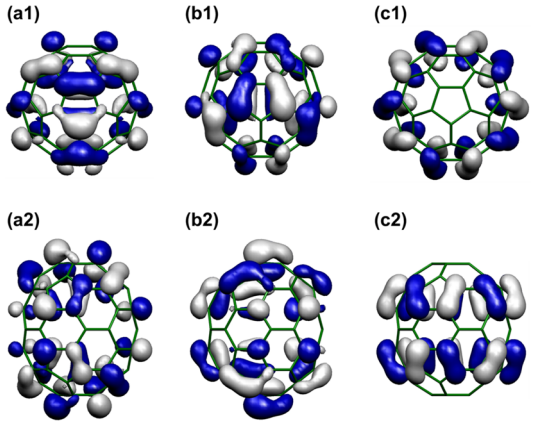

Figure 3. (a1), (a2) top and side views of $e_1''\theta$ LUMO of C_{70}; (b1), (b2) $e_1''\varepsilon$ LUMO; (c1), (c2) a_1'' next LUMO. The isosurface values are 2.0×10^{-2} au. θ denotes the symmetric species with respect to the reflection of the σ_v plane, and ε denotes the antisymmetric species.

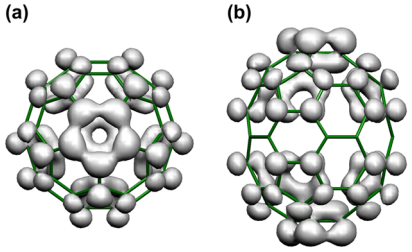

Figure 4. Averaged LUMO density of C_{70}: (a) top view, (b) side view. The isosurface value is 5.0×10^{-4} au.

reported that vibronic coupling density analysis is effective to predict the chemical reactivity of nucleophilic cycloadditions to C_{60}, which is otherwise difficult when employing the frontier orbital theory.[10] In the cycloadditions to C_{60}, the fullerene cage behaves like ethylene. Vibronic coupling density analysis illustrates the existence of six ethylene moieties at the reactive sites. In the present study, we apply vibronic coupling density analysis for nucleophilic cycloadditions to C_{70}. In addition, to discuss the quantitative reactivity, we evaluate the vibronic coupling constants for localized stretching vibrational modes.

2. THEORY

The strength of a vibronic coupling is estimated by a vibronic coupling constant. The linear vibronic coupling constant V_α between an electronic state $|\Psi\rangle$ and a vibrational mode α is defined as

$$V_\alpha := \left\langle \Psi \left| \left(\frac{\partial \hat{H}}{\partial Q_\alpha} \right)_0 \right| \Psi \right\rangle \tag{1}$$

where $\hat{H}$ denotes a molecular Hamiltonian, and Q_α denotes a mass-weighted normal coordinate of mode α. V_α is exactly equal to the integral of a vibronic coupling density $\eta_\alpha(\mathbf{r})$:[8,9]

$$V_\alpha = \int \eta_\alpha(\mathbf{r})\, \mathrm{d}^3\mathbf{r} \tag{2}$$

$\eta_\alpha(\mathbf{r})$ is defined as the product of the electron density difference $\Delta\rho(\mathbf{r})$ between a neutral state and an ionic (charge-transfer) state, and the potential derivative $\nu_\alpha(\mathbf{r})$ with respect to Q_α:

$$\eta_\alpha(\mathbf{r}) := \Delta\rho(\mathbf{r}) \times \nu_\alpha(\mathbf{r}) \tag{3}$$

$\nu_\alpha(\mathbf{r})$ is defined as the derivative of a potential $u(\mathbf{r})$ acting on a single electron from all the nuclei:

$$\nu_\alpha(\mathbf{r}) := \left(\frac{\partial u(\mathbf{r})}{\partial Q_\alpha} \right)_0 \tag{4}$$

$\eta_\alpha(\mathbf{r})$ enables us to discuss the origin of the vibronic coupling in terms of the electronic structure $\Delta\rho(\mathbf{r})$ and the vibrational structure $\nu_\alpha(\mathbf{r})$.

V_α is equal to the gradient of the potential surface in the charge-transfer state along the vibrational mode α. We choose the direction of α such that V_α is negative; that is, the charge-transferred molecule is stabilized with a positive deformation of Q_α.

Parr and Yang have derived the frontier orbital theory on the basis of the conceptual density functional theory, as follows.[11] The ground-state electronic energy of a species S is a functional of the number of electrons N and the potential $u(\mathbf{r})$: $E = E[N,u(\mathbf{r})]$. The chemical potential μ is defined by $(\partial E/\partial N)_u$. The total differential of $\mu = \mu[N,u(\mathbf{r})]$ is written as

$$\mathrm{d}\mu = 2\eta\, \mathrm{d}N + \int f(\mathbf{r})\, \mathrm{d}u(\mathbf{r})\, \mathrm{d}^3\mathbf{r} \tag{5}$$

where η is the absolute hardness

$$\eta := \frac{1}{2}\left(\frac{\partial \mu}{\partial N} \right)_u \tag{6}$$

and $f(\mathbf{r})$ is the Fukui function

$$f(\mathbf{r}) := \left(\frac{\delta \mu}{\delta u(\mathbf{r})} \right)_N = \left(\frac{\partial \rho}{\partial N} \right)_u \tag{7}$$

The main problem related to chemical reactivity is identification of the preferred direction of approach of a reagent R toward a given species S. Parr and Yang assumed that the preferred direction is the one for which the initial $|\mathrm{d}\mu|$ for the species S is a maximum. The Fukui function can be approximated by the frontier orbital density. On the basis of the above principle, they derived the frontier orbital theory.

The present theory is also based on their principle. First, we assume that the Fukui function is approximated by $\Delta\rho(\mathbf{r})$ between a neutral state and an ionic (charge-transfer) state. Second, we assume that the effective mode coincides with the direction of the reaction path. Thus, a reaction coordinate s is defined as

$$\mathrm{d}s := \sum_\alpha \frac{V_\alpha}{\sqrt{\sum_\alpha |V_\alpha|^2}}\, \mathrm{d}Q_\alpha \tag{8}$$

As per the above assumption, $\mathrm{d}u(\mathbf{r})$ can be expressed in terms of $\mathrm{d}s$:

$$\mathrm{d}u(\mathbf{r}) = \left(\frac{\partial u(\mathbf{r})}{\partial s} \right)_0 \mathrm{d}s = \nu_s(\mathbf{r})\, \mathrm{d}s \tag{9}$$

Finally, we obtain

$$\begin{aligned} \mathrm{d}\mu &= 2\eta\, \mathrm{d}N + \int \Delta\rho(\mathbf{r})\nu_s(\mathbf{r})\, \mathrm{d}^3\mathbf{r}\, \mathrm{d}s \\ &= 2\eta\, \mathrm{d}N + \int \eta_s(\mathbf{r})\, \mathrm{d}^3\mathbf{r}\, \mathrm{d}s \end{aligned} \tag{10}$$

where $\nu_s(\mathbf{r})$ and $\eta_s(\mathbf{r})$ are the potential derivative and the vibronic coupling density for the reaction mode s, respectively.

dx.doi.org/10.1021/jo301777d | J. Org. Chem. 2012, 77, 9702−9706

The direction of the effective mode is equal to the steepest descent of the potential surface in the charge-transfer state. Because the deformation along this direction stabilizes the charge-transferred molecule, this direction can be regarded as the preferred direction of the reaction process. The stabilization due to the vibronic couplings originates from a negative contribution of $\eta_s(\mathbf{r})$. From eq 10, $d\mu$ should be small for the preferred direction. Therefore, we modify the original principle by Parr and Yang as follows: the preferred direction is the one for which the initial $d\mu$ for the species S is a minimum, where we replace $|d\mu|$ in the original proposition by $d\mu$. Thus, revival of an analogy of the theory to thermodynamics is possible. Furthermore, we propose the principle in terms of the vibronic coupling density: the preferred direction is the one for which the initial $\eta_s(\mathbf{r})$ for a reaction mode of the species S is a minimum.

The reaction mode should be chosen so as to coincide to the reaction path. However, calculations for a reaction path require considerable amounts of computational resources. In the present study, we seek a practical theory that can predict regioselectivity via a single calculation for an isolated reactant, as in the frontier orbital theory. The effective mode defined by eq 8 may be a candidate for such a reaction mode. For cycloadditions, some localized stretching modes can be also regarded as reaction modes. The localized stretching vibrational vector $\mathbf{v}_{\mathrm{loc}(A,B)}$ of the bond between atom A and atom B is defined as

$$\mathbf{v}_{\mathrm{loc}(A,B)} := \sum_{\xi=x,y,z} \frac{M_B}{\sqrt{M_A^2 + M_B^2}} \frac{R_{A\xi} - R_{B\xi}}{\|\mathbf{R}_A - \mathbf{R}_B\|} \mathbf{e}_{A\xi} - \sum_{\xi=x,y,z} \frac{M_A}{\sqrt{M_A^2 + M_B^2}} \frac{R_{A\xi} - R_{B\xi}}{\|\mathbf{R}_A - \mathbf{R}_B\|} \mathbf{e}_{B\xi} \quad (11)$$

where M_A denotes the mass of nucleus A, and $R_{A\xi}$ is the Ath ξ-component of the molecular geometry $\mathbf{R}$ constructed with N atoms represented by the $3N$-dimensional orthonormal vectors $\{\mathbf{e}_{A\xi}\}$:

$$\mathbf{R} = \sum_A \sum_{\xi=x,y,z} R_{A\xi} \mathbf{e}_{A\xi} \quad (12)$$

$\mathbf{R}_A$ is defined as

$$\mathbf{R}_A := \sum_{\xi=x,y,z} R_{A\xi} \mathbf{e}_{A\xi} \quad (13)$$

The directions of the localized stretching modes are chosen such that the corresponding bonds lengthen. For the case of a diatomic molecule, the localized stretching mode is equal to the normal mode. It should be noted that not all the localized modes are reaction modes. Some of them are introduced as hypothetical reaction modes to evaluate their reactivity.

3. METHOD OF CALCULATION

Because C_{70} is a good electron acceptor as shown in Figure 2, we regard the anionic state as a charge-transfer state. First, we optimized the geometry of C_{70} in the neutral state and performed a vibrational analysis using the RB3LYP/6-311G(d) level of theory. Second, for the optimized geometry, we performed force calculations on the C_{70} anion in the $E_1''\theta$ and $E_1''\varepsilon$ symmetrized electronic states, employing UB3LYP/6-311G(d). GAUSSIAN 09[12] was used for these calculations. For the $E_1''\theta$ and $E_1''\varepsilon$ anionic states, we calculated the vibronic coupling constants and the vibronic coupling densities for their effective modes by employing our programs. Furthermore, for both the states, we calculated the vibronic coupling constants for the localized stretching modes at all the C−C bonds.

Because of the selection rule, the E_1'' electronic state couples with only a_1' modes and e_2' modes ($[E_1''^2] = a_1' \oplus e_2'$). Therefore, the effective mode for the E_1'' electronic state consists of a_1' modes and e_2' modes. Since the molecular distortion along these modes does not cause mixing of the E_1'' electronic configurations with the A_1'' electronic configuration ($a_1'e_2' \not\subset E_1'' \otimes A_1'' = e_1'$), the low-lying A_1'' first excited electronic configuration is not taken account in the present calculations. The pseudo Jahn−Teller effect via the e_1' modes is discussed in Appendix A of Supporting Information.

4. RESULTS AND DISCUSSION

Figures 5 and 6 show the electron density differences $\Delta\rho(\mathbf{r})$, effective modes s, and potential derivatives $\nu_s(\mathbf{r})$ for the $E_1''\theta$ and $E_1''\varepsilon$ electronic states, respectively. The electron density differences $\Delta\rho(\mathbf{r})$ involve the positive contribution from the LUMOs of C_{70} as well as the negative contribution from the other orbitals. As shown in Figures 5b and 6b, the effective modes cause elongation of the a−b and c−c bonds but shortening of the a−a and b−c bonds. We classify the elongated a−b and c−c bonds as type-L, and the shortened a−a and b−c bonds as type-S. In the cycloadditions to C_{70}, the C−C bond lengths at the reactive sites increase. Therefore, type-L C−C bonds can be reactive sites, and type-S C−C bonds can be unreactive sites.

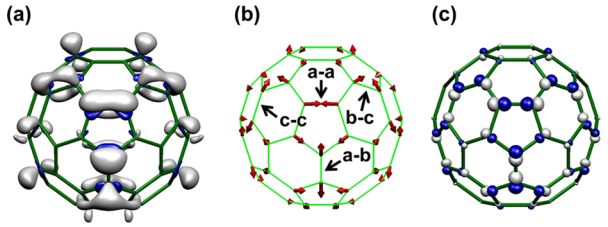

Figure 5. (a) Electron density difference $\Delta\rho(\mathbf{r})$ (the isosurface value is 1.0×10^{-3} au), (b) effective mode s, and (c) potential derivative $\nu_s(\mathbf{r})$ (the isosurface value is 1.0×10^{-2} au) for the $E_1''\theta$ state. The white and blue regions indicate positive and negative, respectively.

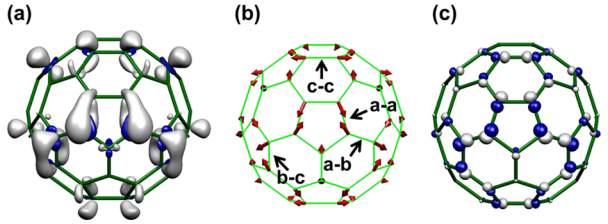

Figure 6. (a) Electron density difference $\Delta\rho(\mathbf{r})$ (the isosurface value is 1.0×10^{-3} au), (b) effective mode s, and (c) potential derivative $\nu_s(\mathbf{r})$ (the isosurface value is 1.0×10^{-2} au), for the $E_1''\varepsilon$ state. The white and blue regions indicate positive and negative, respectively.

Figure 7 shows the vibronic coupling densities $\eta_s(\mathbf{r})$ for the $E_1''\theta$ and $E_1''\varepsilon$ electronic states. As shown in Figure 7, the vibronic coupling densities $\eta_s(\mathbf{r})$ have large negative values at the type-L and type-S bonds, and their forms are different from each other. In the previous study, we found that the ethylene moieties were at the same sites as the reactive sites in C_{60} on the basis of the vibronic coupling density.[10] Therefore, we can expect some ethylene moieties in the present system, C_{70}, as well. For comparison, Figures 8a and 8b show the vibronic coupling densities $\eta_s(\mathbf{r})$ for the ethylene anion at the reactive sites of C_{70} which was reported by the experiments. $\eta_s(\mathbf{r})$ for

dx.doi.org/10.1021/jo301777d | J. Org. Chem. 2012, 77, 9702−9706

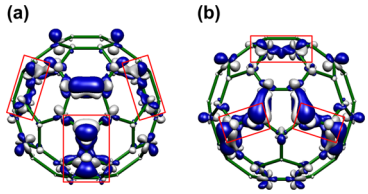

Figure 7. (a) Vibronic coupling densities $\eta_s(\mathbf{r})$ for the $E_1''\theta$ state, and (b) for the $E_1''\varepsilon$ state. The isosurface values are 3.0×10^{-6} au. The white and blue regions indicate positive and negative, respectively. Red boxes show ethylene moieties embedded in the reactive sites (see Figure 8 for comparison).

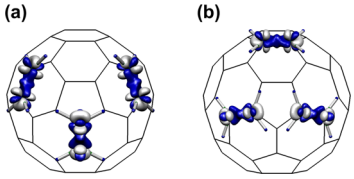

Figure 8. Vibronic coupling densities $\eta_s(\mathbf{r})$ for ethylene anion placed on the C_{70} frame. The isosurface values are 2.0×10^{-4} au. The white and blue regions indicate positive and negative, respectively. For comparison, see Figure 7 in which the ethylene moieties embedded in the C_{70} anion is shown by red boxes.

C_{70} anion at the type-L a–b bonds, which are elongated by the longest displacement in the effective modes, is similar to that for the ethylene anion, as has been observed for C_{60}.[10] Vibronic coupling density analysis reveals that the reactive sites in fullerenes bear ethylene moieties as functional groups. These results support the principle that the preferred direction is the one for which the initial $\eta_s(\mathbf{r})$ for the species S is a minimum.

Furthermore, for a quantitative evaluation of the regioselectivity of C_{70}, we estimated vibronic coupling constants for the localized stretching vibrational modes. The localized stretching mode is defined in eq 11, and an example is shown in Figure 9a. The direction of the localized stretching

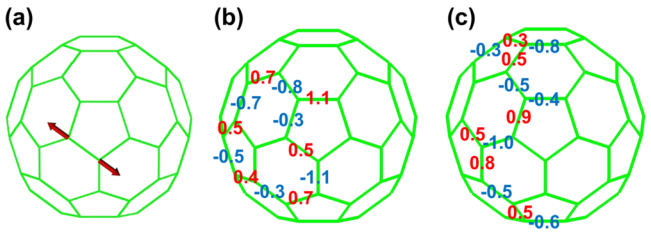

Figure 9. (a) A localized stretching vibrational mode at one of the a–a bonds, (b) the vibronic coupling constants/10^{-4} au for localized stretching modes in the $E_1''\theta$ electronic state, and (c) in the $E_1''\varepsilon$ electronic state. Vibronic coupling constants whose absolute values are smaller than 0.25×10^{-4} au are ignored.

mode is chosen such that the corresponding C–C bond becomes longer. As shown in Figures 9b and 9c, the vibronic coupling constants for the localized stretching modes assume negative values at the type-L bonds and positive values at the type-S bonds. The vibronic coupling constants for the localized stretching modes indicate the magnitudes of the vibronic coupling density for the effective mode at the corresponding C–C bonds. In addition, the vibronic coupling constants for the localized stretching modes can be averaged over all the E_1'' electronic states (see Appendix B of Supporting Information). Because of the invariance of the averaged vibronic coupling constants under unitary transformation, it is appropriate to consider them as reactivity indices. Table 1 lists the averaged

Table 1. Averaged Vibronic Coupling Constant for the Localized Stretching Mode at Each Type of C–C Bond[a]

type of C–C bond	averaged vibronic coupling constant/10^{-4} au
a–a	0.316
a–b	−0.782
b–c	0.339
c–c	−0.442
c–d	0.123
d–d	−0.209
d–e	0.031
e–e	−0.024

[a]The labeling is defined in Figure 1.

vibronic coupling constant for the localized stretching mode at each type of C–C bond. As shown in Table 1, the averaged vibronic coupling constants for the localized stretching modes at the a–b bonds and c–c bonds have the largest and second largest negative values, respectively. Therefore, in terms of vibronic couplings, these bonds can be concluded to be the most and second most reactive sites. This result agrees well with the regioselectivity observed in the experiments.[1−3] In contrast to the frontier orbital theory, the present approach does not depend on the selection from the degenerate e_1'' LUMOs; that is, this approach is invariant under any unitary transformation. This is one of the advantages of our approach over the frontier orbital theory.

The type-S and type-L bonds indicated by the effective mode correspond to the phase of the e_1'' LUMO into which an electron is added, that is, whether the LUMO is bonding or antibonding. However, we can choose $e_1''\theta$ LUMO, $e_1''\varepsilon$ LUMO, or a mixture of the two. As shown in Figure 3, we can choose the e_1'' LUMO such that it is either bonding or antibonding, for example, at one of the a–a bonds. It should be noted that the orbital phase chosen is arbitrary in degenerate systems. The averaged vibronic coupling constants for localized stretching modes are free of this problem and hence help in extending the frontier orbital theory[4,5] to degenerate systems.

5. CONCLUSION

The vibronic coupling density for the effective mode illustrates both the reactive and unreactive sites of C_{70}. From vibronic coupling density analysis, as in the case of C_{60}, the C_{70} cage is found to bear ethylene moieties at the reactive sites as functional groups. In other words, the reactive sites of C_{70} attacked by nucleophiles have a large electron density difference $\Delta\rho$ and large displacements in the molecular vibrations, both of which are similar to those for ethylene. Furthermore, the averaged vibronic coupling constant for the localized stretching mode, which is invariant under unitary transformation, enables us to discuss the reactivity of each C–C bond of C_{70} quantitatively. The calculated results agree well with the regioselectivity reported by the experiments. Using the averaged vibronic coupling constants, we can predict the regioselectivity of various reactants even if the frontier orbitals are degenerate.

The averaged vibronic coupling constant for the localized mode is equal to one-half of the trace of a vibronic coupling matrix, that is, one-half of the sum of $\langle\theta|(\partial\hat{H}/\partial Q_\alpha)_0|\theta\rangle$ and $\langle\varepsilon|(\partial\hat{H}/\partial Q_\alpha)_0|\varepsilon\rangle$, where $|\theta\rangle$ and $|\varepsilon\rangle$ denote the $E_1''\theta$ and $E_1''\varepsilon$

dx.doi.org/10.1021/jo301777d | J. Org. Chem. 2012, 77, 9702–9706

anionic states, respectively. We neglected the off-diagonal elements, $\langle\theta|(\partial\hat{H}/\partial Q_\alpha)_0|\varepsilon\rangle$ and $\langle\varepsilon|(\partial\hat{H}/\partial Q_\alpha)_0|\theta\rangle$. Although we can define another averaged value including the off-diagonal elements, it has a different physical meaning and is not suitable for chemical reactivity discussions. We will publish the difference between the two types of the averaged values and the physical meaning of the off-diagonal elements from the viewpoint of the Jahn−Teller theory in the near future.

In terms of vibronic coupling density, we can modify the principle proposed by Parr and Yang as follows: the preferred direction is the one for which the initial $\eta_s(\mathbf{r})$ for a reaction mode of the isolated reactant is a minimum. It is necessary to verify the present principle by applying the vibronic coupling density analysis to other reactions. In the near future, we will report the results of cycloadditions to other higher fullerenes[1] and endohedral fullerenes,[13] as well as the results of other attractive reactions.

■ ASSOCIATED CONTENT

Supporting Information

Appendix A on the pseudo Jahn−Teller effect of the low-lying A_1'' anionic state of C_{70}. Appendix B on the averaged vibronic coupling constant. Computational details, including tables on the optimized geometry of neutral C_{70}, total electronic energies of C_{70} and its anion, and the effective modes for the anionic states. This material is available free of charge via the Internet at http://pubs.acs.org.

■ AUTHOR INFORMATION

Corresponding Author

*E-mail: tsato@moleng.kyoto-u.ac.jp.

Notes

The authors declare no competing financial interest.

■ ACKNOWLEDGMENTS

Numerical calculations were performed partly in the Supercomputer Laboratory of Kyoto University and Research Center for Computational Science, Okazaki, Japan. This research was also supported in part by the Global COE Program "International Center for Integrated Research and Advanced Education in Materials Science" (no. B-09) of the Ministry of Education, Culture, Sports, Science and Technology (MEXT) of Japan, administered by the Japan Society for the Promotion of Science.

■ REFERENCES

(1) Thilgen, C.; Diederich, F. *Chem. Rev.* **2006**, *106*, 5049−5135.
(2) Herrmann, A.; Diederich, F.; Thilgen, C.; ter Meer, H.-U.; Muller, W. H. *Helv. Chim. Acta* **1994**, *77*, 1689−1706.
(3) Meier, M. S.; Poplawska, M.; Compton, A. L.; Shaw, J. P.; Selegue, J. P.; Guarr, T. F. *J. Am. Chem. Soc.* **1994**, *116*, 7044−7048.
(4) Fukui, K.; Yonezawa, T.; Shingu, H. *J. Chem. Phys.* **1952**, *20*, 722−725.
(5) Fukui, K. *Acc. Chem. Res.* **1971**, *4*, 57−64.
(6) Fischer, G. *Vibronic Coupling: The Interaction between the Electronic and Nuclear Motions*; Academic Press: London, 1984.
(7) Bersuker, I. *The Jahn-Teller Effect*; Cambridge University Press: Cambridge, 2006.
(8) Sato, T.; Tokunaga, K.; Tanaka, K. *J. Phys. Chem. A* **2008**, *112*, 758−767.
(9) Sato, T.; Tokunaga, K.; Iwahara, N.; Shizu, K.; Tanaka, K. In *The Jahn-Teller Effect: Fundamentals and Implications for Physics and Chemistry*; Köppel, H., Yarkony, D. R., Barentzen, H., Eds.; Springer−Verlag: Berlin, 2009.
(10) Sato, T.; Iwahara, N.; Haruta, N.; Tanaka, K. *Chem. Phys. Lett.* **2012**, *531*, 257−260.
(11) Parr, R. G.; Yang, W. *J. Am. Chem. Soc.* **1984**, *106*, 4049−4050.
(12) Frisch, M. J. et al. *Gaussian 09, Revision B.01*; Gaussian, Inc., Wallingford, CT, 2009.
(13) Lu, X.; Akasaka, T.; Nagase, S. *Chem. Commun.* **2011**, *47*, 5942−5957.